Flow Acceleration in an RDRE with Gradual Chamber Constriction

Mathias C. Ross
University of California at Los Angeles
Los Angeles, CA, USA
&
Jason Burr, Armani Batista, Christopher Lietz
Air Force Research Laboratory
Edwards AFB, CA, USA

1 Introduction

Rotating detonation rocket engine (RDRE) technology has matured in recent years, and only a few hurdles remain before they're ready to be used in practical devices. This was emphasized recently by the Japan Aerospace Exploration Agency (JAXA), which successfully tested an RDRE as the upper stage of a sounding rocket [1]. However, there's still work that needs to be done in designing nozzles that get the most out of a detonation device; unfortunately, this is not a straightforward problem. Progress has been made toward optimally accelerating a time-varying flow at the exit of a rotating detonation combustor [2], but it has also been shown that the design of a nozzle affects the chamber dynamics themselves [3] – meaning the nozzle design is coupled with the incoming flow to be optimized. Understanding the connection between nozzle design and detonation behavior will be critical as the community continues to improve RDRE design.

The present work examines two high fidelity large eddy simulations of a gaseous methane-oxygen RDRE. One is based on the prototypical annular detonation engine design, with an unconstricted channel that exhausts over a straight aerospike. The second simulation considers the same flow conditions, but instead uses a chamber with a gradual constricting section, resulting in a converging-diverging nozzle. The simulations are based on experimental results [4] that show the gradual constriction has a large impact on detonation behavior, and the present work tracks the energy content of the flow to consider the large scale differences that exist between an unconstricted RDRE chamber and one with a gradual constriction.

2 Case Setup

The present study is a follow-up to an Air Force Research Laboratory (AFRL) RDRE testing campaign, in which a gaseous methane-oxygen RDRE was tested for a variety of flow conditions [4]. We have selected two specific test cases from the study, both using a 76 mm combustion chamber, 33 mm inner radius, and 5 mm channel width. In the unconstricted case the channel remains 5 mm wide over the entire length; however, in the constricted geometry the inner body is shaped to turn the flow 4.4 degrees, culminating in a 2 mm wide throat 65 mm from the injection plane.

Correspondence to: rossmathiasc@ucla.edu

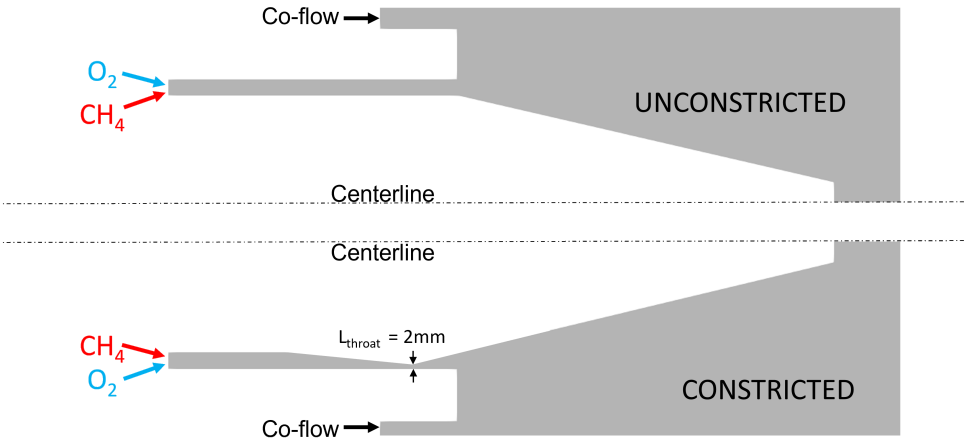

Figure 1: Domain diagram, with simplified injector geometry, for both an unconstricted geometry (top) and a chamber with a gradual constriction (bottom).

Table 1: Boundary conditions enforced at flow inlets and outlets.

Enforced Condition	**Value**
Fuel Mass Flux (kg/s)	0.06
Fuel Temperature (K)	300
Oxidizer Mass Flux (kg/s)	0.21
Oxidizer Temperature (K)	300
Co-flow Velocity (m/s)	1
Co-flow Temperature (K)	300
Subsonic Outflow Pressure (Pa)	9.2×10^4

A simplified diagram of the engine geometry is shown in figure 1, showing what is modeled by the simulation mesh. The injector specifics are not included in the diagram, but both simulation domains include the full injector geometry: 72 discrete impinging injector pairs, connected to upstream injection plenums.

The FFCMy-12 mechanism, which tracks 12 species and 38 reactions [5], was used to model reaction chemistry, and the simulation was run using the ALREST (Advanced Liquid-Rocket Engine Scaling Tool) High-Fidelity Modeling (AHFM) framework – which is built on the Large Eddy Simulation with Linear Eddy (LESLIE) code developed at the Georgia Institute of Technology. Non-slip, adiabatic boundary conditions are enforced at the engine walls, with slip conditions at the walls of the downstream exhaust plenum. Although adiabatic wall conditions are commonly used in RDRE simulations, the absence of a heat-loss mechanism may have a large impact on global performance metrics; the adiabatic assumption in particular has been estimated to reduce overall enthalpy loss by 13% for short-duration simulations [6]. Boundary conditions at the inlets and exit were chosen to produce a methane/oxygen equivalence ratio (ϕ) of 1.1, and a mass flux ($\dot{m}$) of 0.27 kg/s; enforced parameters are listed in Table 1. In all, each mesh consisted of approximately 136M cells, and each case used 5M CPU hours to simulate the first 2.0 ms of physical time. For more information on the specifics of these simulations, see [7].

Table 2: Summary of quasi-steady mode achieved in both simulations. Counter-propagating waves were sustained in the constricted case, and so number and wavespeeds are separated by direction in that case. Pressure (Press.) 1 is an average measurement 9 mm from the injection plane, and Press. 2 is the same measurement 29 mm from the injection plane, locations chosen to coincide with experimental capillary tube attenuated pressure locations in Bennewitz et al. [4].

	# of waves	Wavespeeds (m/s)	Press. 1 (MPa)	Press. 2 (MPa)	Thrust (N)	I_{sp} (s)
Unconstricted	3/-	1660/-	0.43	0.34	513	189
Constricted	8/8	1330/1280	1.06	1.05	629	231

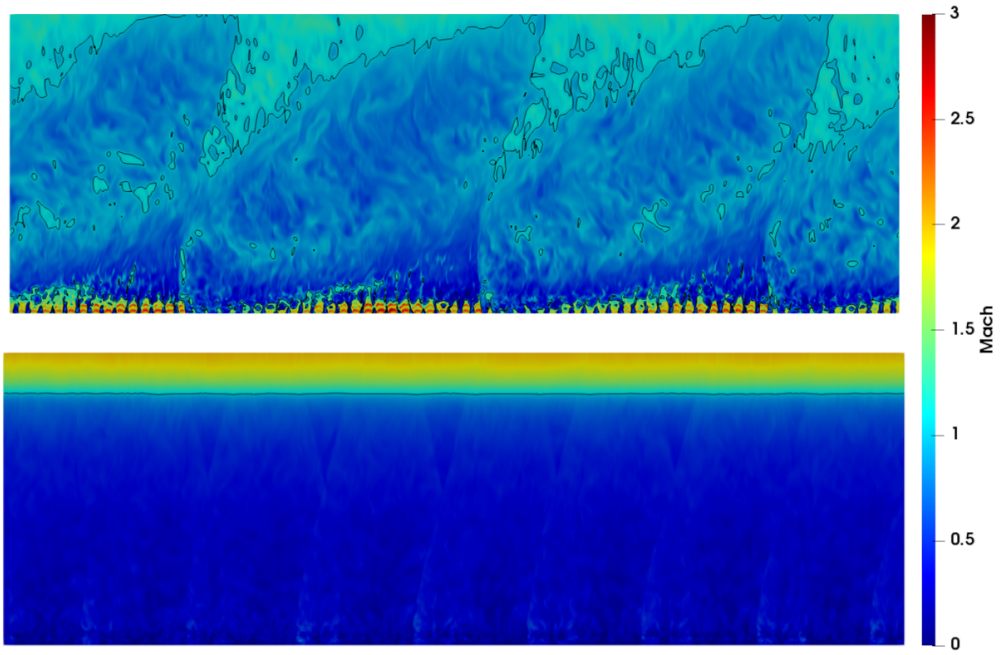

Figure 2: Chamber Mach fields, for the center-channel of an unconstricted RDRE (top) and the throat-center of a constricted RDRE (bottom). Black line represents sonic isocontour.

3 Results and Analysis

A summary of the quasi-steady-state conditions attained in the simulation is shown in table 2. Unsurprisingly, the nozzle increased thrust and I_{sp}, while also increasing pressure inside of the chamber. These simulations also captured an effect seen experimentally, that an RDRE with a nozzle may sustain counter-propagating modes not present in an unconstricted geometry at the same flow conditions.

3.1 Mach Fields

In an unconstricted RDRE, the flow goes supersonic in pockets behind the oblique shock structure. This is consistent with the 2D results of Zhdan et al. [8], and has been seen in other numerical works. In a case of this sort, after encountering a detonation the flow begins to expand as it travels axially towards the chamber exit, and reaches Mach 1 after encountering the oblique shock.

It is worth noting that in this simulation a large exhaust region is included in the simulation domain, and so there is no numerical condition forcing the flow to reach Mach 1 at the exit of the chamber. The

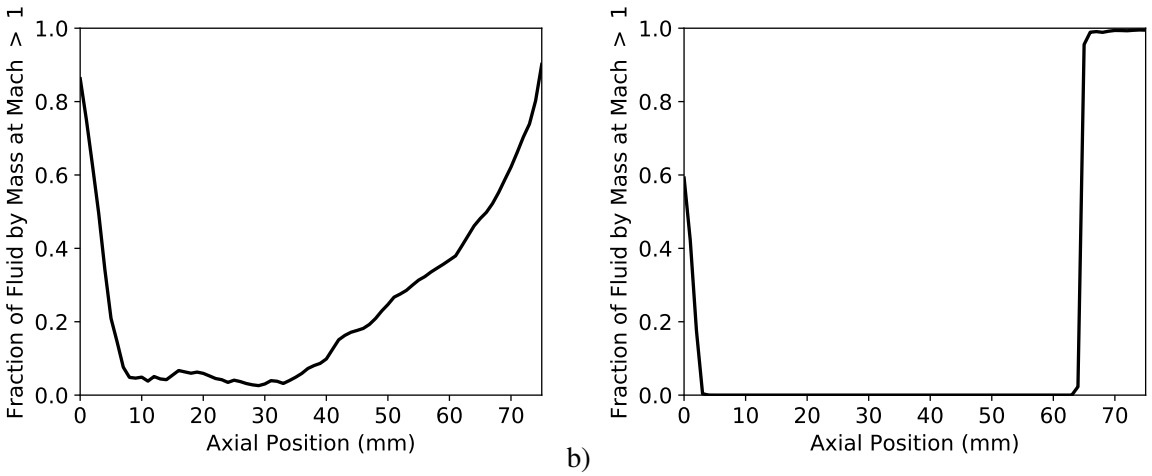

Figure 3: Instantaneous fraction of the flow which is supersonic at each axial position for a) an unconstricted RDRE and b) a constricted RDRE. Fraction of total mass flux is defined in equation 1.

amount of the flow which chokes before leaving the engine is indicated in Fig. 3, which shows the percentage of the flow which is supersonic at each axial location,

$$\frac{\int_{A_{supersonic}} \rho u \, dA_{supersonic}}{\int_A \rho u \, dA} \tag{1}$$

In this case the majority of the flow is thermally choked before reaching the exit of the chamber – however, this field suggests that an engine with a shorter length may be largely subsonic at the chamber exit.

In both cases there exists a region of supersonic flow near the injection region of the chamber. This is a consequence of reactants undergoing choked injection followed by expansion inside the chamber, and near the injection plane it accounts for the majority of the flow's kinetic energy.

In the case of a gradual constriction, the flow reaches Mach 1 only at the physical throat. Unlike in the unconstricted case, there are no pockets of supersonic flow behind the oblique shock – the flow transitions in its entirety from subsonic to supersonic at the physical throat location; this is a direct application of the classical Mach-Area relationship, which requires that the cross-sectional area be neither increasing nor decreasing when the flow reaches the sonic condition.

That this holds so completely for an RDRE shows a fundamental difference between designs with and without a gradual constriction: the gradual constriction changes the acoustic conditions of the chamber, effectively enforcing an acoustic length in the axial direction in accordance with the throat. This is something that needs to be taken into account when considering the detonation dynamics of an RDRE – while the severity of a constriction may change properties of reflected shock waves traveling into the chamber, this means a gradual constriction can affect detonation dynamics even without considering reflections of the oblique shock structure. Although there are complicated dynamics associated with constricted RDRE detonations, this effect may provide utility when designing a practical device; moreover, the complete choking with a gradual constriction is useful when designing simulations that require supersonic boundary conditions.

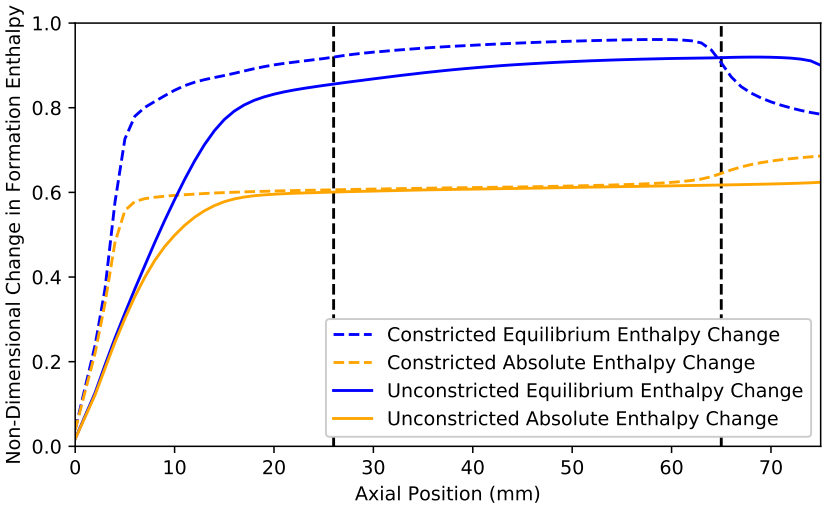

Figure 4: Change in enthalpy of formation of the two geometries, given in non-dimensional forms scaled against idealized combustion and compared to equilibrium conditions. Vertical lines at 26 mm and 65 mm indicate constriction start and constriction throat, respectively.

3.2 Enthalpy Conversion

A nozzle's acceleration of the flow increases thrust, and so it becomes difficult to determine to what extent the performance of an RDRE with a nozzle is affected by any change in detonation dynamics. One way to approach this is to consider what is meant by performance: on a fundamental level, the goal of a rocket engine is to convert the propellant's latent energy into a kinetic form. In a simulation, this conversion can be tracked directly by considering the change in formation enthalpy inside the chamber.

Figure 4 represents this change in formation enthalpy in two ways for each of the geometries. The first – which we'll call the "absolute" form – is the overall change in formation enthalpy, non-dimensionalized using the enthalpy released in an idealized one-step total combustion: $CH_4 + 2\,O_2 \longrightarrow 2\,H_2O + CO_2$. For species s, density ρ, velocity $\vec{u}$, mass fraction Y_s, molar mass μ_s, and formation enthalpy per mol h_s^0, in a fuel-rich engine flowing $\dot{N}_{O_2}$, and $\dot{N}_{CH_4}$ moles per second of O_2 and CH_4 respectively, this can be written out over a surface:

$$\Delta\hat{h}_{cc} = -\frac{\int_{S_{\text{out}}} \sum_s \left(\frac{Y_s}{\mu_s} h_s^0\right) \rho\vec{u} \cdot d\vec{S} - \left(\dot{N}_{CH_4} h_{CH_4}^0 + \dot{N}_{O_2} h_{O_2}^0\right)}{\left[\dot{N}_{O_2} h_{H_2O}^0 + \frac{1}{2}\dot{N}_{O_2} h_{CO2}^0 + \left(\dot{N}_{CH_4} - \frac{1}{2}\dot{N}_{O_2}\right) h_{CH_4}^0\right] - \left(\dot{N}_{CH_4} h_{CH_4}^0 + \dot{N}_{O_2} h_{O_2}^0\right)} \tag{2}$$

In this form, an absolute formation enthalpy change ($\Delta\hat{h}_{cc}^0$) of 0 means that no energy has been extracted from combustion, while a value of 1 indicates that all of the energy released by an (extremely) ideal conversion of methane and oxygen to water and carbon dioxide has been extracted.

Tracking this absolute form in Fig. 4, it can be seen that both geometries reach a value just under 0.6 within the first 20 mm of the chamber, and then stay nearly constant for much of the remaining length. Both cases have the same change in formation enthalpy after the detonation zone, meaning that both cases extract the same amount of energy through combustion. This is counter to the normal expectation that combusting at a higher chamber pressure would release more energy; instead, the change in combustion behavior observed with the addition of a constriction counteracts the anticipated increase in energy release due to the increase in pressure. The tracked change in formation enthalpy thus pro-

vides an indication that the development of counter-propagating behavior brings the engine further from operating according to an ideal detonation engine cycle.

When considering the completeness of combustion, it is often preferable to compare to a possible equilibrium condition instead of to the overall ideal. A metric of this sort is given in Fig. 4, where "equilibrium efficiency" refers to the non-dimensional value obtained by replacing the denominator in equation 2 with the enthalpy that would have been released if the flow was allowed to equilibrate. This quantity was calculated using Cantera for local conditions for the values shown in Fig. 4. In this form a zero again means that no energy has been released due to combustion, but a one means that the combustion reaction is as complete as is possible for the local equilibrium conditions. The higher pressure and temperature in the constricted case means that, for the same energy released from combustion, the flow is closer to the local equilibrium conditions. However, near the throat the nozzle acceleration is large enough to partially freeze the flow – bringing the amount of released energy further from what would occur at the local equilibrium condition. The sonic condition in the constricted case occurs at the throat, and so instead of comparing the equivalent axial location between the two geometries it makes sense to compare the sonic location of 76 mm in the unconstricted case to 65 mm in the constricted case – at which location the equilibrium change in absolute enthalpy is the same in both cases. This is an indication that the change in performance in the two cases cannot be attributed to a difference in combustion completeness; instead, the increased thrust in the constricted case is just due to the nozzle's acceleration of the flow.

4 Conclusions

Even a gradual constriction is enough to force choking locations to a specific axial location in an RDRE, which is important when considering acoustic boundaries and can potentially be leveraged in future designs. For this simple nozzle, tracking formation enthalpy shows that, although the change in geometry leads to an increased chamber pressure, the accompanying change in detonation dynamics prevents a net improvement in completeness of combustion in the chamber. This analysis shows that this nozzle design is far from ideal for an RDRE, and the connection between detonation dynamics and a downstream constriction impacts the engine's ability to leverage the benefits of pressure gain combustion.

5 Acknowledgments

This work has been supported by the Air Force Office of Scientific Research (AFOSR), under AFRL Lab Task 20RQCOR63 funded by the AFOSR Energy, Combustion, and Non-Equilibrium Thermodynamics portfolio with Dr. Chiping Li as program manager. Additionally, the work was supported in part by high-performance computer time and resources from the DoD High Performance Computing Modernization Program.

References

[1] K. Goto, K. Matsuoka, K. Matsuyama, A. Kawasaki, H. Watanabe, N. Itouyama, K. Ishihara, V. Buyakofu, T. Noda, J. Kasahara, A. Matsuo, I. Funaki, D. Nakata, M. Uchiumi, H. Habu, S. Takeuchi, S. Arakawa, J. Masuda, K. Maehara, T. Nakao, and K. Yamada, "Flight Demonstration of Detonation Engine System Using Sounding Rocket S-520-31: Performance of Rotating Detonation Engine," in *AIAA SCITECH 2022 Forum*. San Diego, CA &

Virtual: American Institute of Aeronautics and Astronautics, Jan. 2022. [Online]. Available: https://arc.aiaa.org/doi/10.2514/6.2022-0232

[2] K. Miki, D. E. Paxson, D. Perkins, and S. Yungster, "RDE Nozzle Computational Design Methodology Development and Application," ser. AIAA Propulsion and Energy 2020 Forum, Aug. 2020.

[3] R. Bluemner, C. Paschereit, E. Gutmark, and M. Bohon, "Investigation of Longitudinal Operating Modes in Rotating Detonation Combustors," ser. AIAA Scitech 2020 Forum, Jan. 2020.

[4] J. W. Bennewitz, B. R. Bigler, M. C. Ross, S. A. Danczyk, W. A. Hargus, and R. D. Smith, "Performance of a Rotating Detonation Rocket Engine with Various Convergent Nozzles and Chamber Lengths," *Energies*, vol. 14, no. 8, p. 2037, Jan. 2021, number: 8 Publisher: Multidisciplinary Digital Publishing Institute. [Online]. Available: https://www.mdpi.com/1996-1073/14/8/2037

[5] G. P. Smith, Y. Tao, and H. Wang, "Foundational Fuel Chemistry Model Version 1.0 (FFCM-1)," 2016. [Online]. Available: http://nanoenergy.stanford.edu/ffcm1

[6] P. Strakey, D. Ferguson, A. Sisler, and A. Nix, "Computationally Quantifying Loss Mechanisms in a Rotating Detonation Engine," in *54th AIAA Aerospace Sciences Meeting*. San Diego, California, USA: American Institute of Aeronautics and Astronautics, Jan. 2016. [Online]. Available: https://arc.aiaa.org/doi/10.2514/6.2016-0900

[7] C. Lietz, M. Ross, Y. Desai, and W. Hargus, "Numerical investigation of operational performance in a methane-oxygen rotating detonation rocket engine," ser. AIAA Scitech 2020 Forum, Jan. 2020.

[8] S. A. Zhdan, F. A. Bykovskii, and E. F. Vedernikov, "Mathematical Modeling of a Rotating Detonation Wave in a Hydrogen-Oxygen Mixture," *Combustion, Explosion, and Shock Waves*, vol. 43, no. 4, pp. 449–459, 2007.